

Full-scale Pile Load Tests using Osterberg Cells in Meta-sedimentary Rock

Alvin K.M. Lam, Andrew T.F. Wong & Zoe S.T. Leung

Ove Arup & Partners Hong Kong Limited, Hong Kong

Sylvia S.W. Chik, Kian Y.K. Chiu, Eric H.Y. Sze,

Patrick P.C. Wong & Thomas H.H. Hui

Geotechnical Engineering Office,

Civil Engineering and Development Department,

Government of the Hong Kong Special Administrative Region,

Hong Kong SAR, China

Andy Y.F. Leung

Hong Kong Polytechnic University, Hong Kong

doi: <https://doi.org/10.21467/proceedings.7.7.29>

ABSTRACT

Meta-sedimentary (MS) rocks are the dominant geological formation in the northern district of Hong Kong, an area earmarked for extensive urban development in the upcoming decades. This geological context presents challenges for foundation design, as existing practices typically employ conservative design parameters for piles founded in these formations. To investigate opportunities for optimisation, a series of full-scale pile load tests utilising Osterberg Cells (O-cells) combining with the loading kentledge have recently been conducted. The O-cell method integrates a sacrificial hydraulic jack at the base of the test pile enabling direct transfer of applied load to the rock for accurate measurement of both rock socket friction and end-bearing resistance. Unlike traditional pile load tests by loading kentledge, this eliminates the uncertainty of load shedding to the ground above the rock socket. Furthermore, the experience of using fibre optic technology for real-time strain measurements during the tests will be discussed. This novel approach is rigorously evaluated against the traditional vibrating wire strain gauge with a view to assessing the operational accuracy and overall efficiency of both techniques. The first batch of test piles has been carried out in Yuen Long South and Long Bin. This paper presents details of the test set-up, the loading sequence, the load-movement behavior of the test piles and the mobilised end-bearing capacity in the MS rocks. Rock Mass Rating (RMR) of the MS rocks at the founding levels have been determined, based on information obtained from ground investigation or pre-drill boreholes. The evaluation method of RMR and its applicability will be discussed. The findings of this study contribute valuable insights for future instrumented pile load tests in Hong Kong.

1 INTRODUCTION

Meta-sedimentary (MS) rocks are the predominant geological formation in the northern districts of Hong Kong, including areas within the planned Northern Metropolis, where substantial infrastructure and urban development are anticipated in the coming decades. However, foundation design in MS rocks remains constrained by conservative parameters prescribed in local codes of practice, particularly with regard to the allowable end-bearing pressures and socket bond resistance. It is mainly due to the general lack of geotechnical data for MS rocks in the past. These cautious design assumptions often result in conservative and costly pile foundation works and longer construction time, potentially impeding efficient land development in the region.

While there have been notable local precedents of pile testing in MS rocks, including test piles conducted during the Kowloon-Canton Railway Corporation (KCRC) West Rail Project Phase 1, these data remain limited in scale and applicability. Nevertheless, they provided useful insights into rock socket friction and end-bearing



capacity, but a more systematic and instrumented approach is needed to enhance confidence in design parameters, particularly for deep foundations subject to complex geological variability.

Recognising the need to optimise pile design in MS rocks, the Geotechnical Engineering Office (GEO) has launched a full-scale pile testing programme using Osterberg Cells (O-cells) for bi-directional loading. Tests were first conducted at two trial sites in Yuen Long South and Long Bin with comprehensive instrumentation including vibrating wire gauges and fibre optic sensors. Geological conditions were assessed using borehole data and Rock Mass Rating (RMR) classification. This paper presents the details of the test pile design, construction, instrumentation, and testing procedures, followed by interpretation of load-movement behavior and assessment of mobilised end-bearing capacities. The effectiveness of fibre optic technology for real-time strain monitoring is evaluated through comparison with traditional instrumentation. The results of the pile load tests have provided valuable insights into the actual performance of piles in MS rocks under controlled loading conditions, which are vital for the formulation of future foundation design guidelines to support developments in the Northern Metropolis. The overall study plan for reviewing the foundation design of MS rocks is documented in Chik et al. (2025).

2 DESIGN PRACTICE FOR META-SEDIMENTARY ROCKS IN HONG KONG

2.1 Geological Challenges

MS rocks are sedimentary rocks subjected to metamorphism. It is very common to find the presence of closely spaced rock joints in MS rocks in Hong Kong rendering the difficulty of gathering full diameter rock core samples for conducting the conventional Unconfined Compressive Strength (UCS) and/or point load tests to verify the rock strength. In some cases, the rock is so fragmented that it becomes non-intact. Some geologists may describe the non-intact material as Grade IV material. If the thickness is substantial, this will have a major implication to define the engineering bedrock for load bearing piles. Therefore, the feasibility of using irregular lump point load test to determine the strength of MS rocks should be explored.

2.2 Design Practice

In Hong Kong, the Buildings Department (BD) published the Code of Practice for Foundations 2017 (2024 Edition), which classifies MS rocks as Category 2 rock. For moderately decomposed, moderately strong to moderately weak MS rocks of material weathering grade III or better, and with not less than 85% total core recovery (TCR) of the designated grade, a presumed allowable bearing pressure of 3,000 kPa can be adopted. It is noteworthy that there is no specific requirement on the intact rock strength of MS rocks. A presumed allowable bond or friction between rock and concrete or grout of 300 kPa and 150 kPa can be adopted for piles under compression/transient tension and permanent tension respectively. Comparing with igneous rocks, the presumed allowable bearing pressure and bond/friction of MS rocks are much lower than those for igneous rocks. Therefore, GEO has initiated a systematic pile load testing programme to investigate the potential to uplift the presumed allowable bearing pressure and bond/friction of MS rocks, with a view to producing a more cost-effective foundation designs in MS rocks.

2.3 Use of Rock Mass Rating Method

According to Table 6.5 of GEO (2006), the allowable bearing capacity of a pile resting on a jointed rock mass can be evaluated by assessing the respective Rock Mass Rating (RMR). For example, an allowable bearing capacity of 5,000 kPa could be adopted for rock mass with RMR value of 50, and that 14,500 kPa for rock mass with RMR value of 88 (i.e. the maximum value). The RMR method, developed by Bieniawski (1973) and (1989), is a tool to assess the properties of rock mass. Five parameters are considered including the strength of intact rock, Rock Quality Designation (RQD), spacing of joints, conditions of joints and groundwater. The strength is usually determined by UCS or point load test. The joint spacing can be calculated using the fracture index while the condition of joints can be assessed based on visual inspections of the retrieved rock cores and/or the descriptions of the borehole logs. In the current practice, the RMR value shall be assessed to depth of not less than three times the diameter of the pile base. For more details about the RMR method and its potential enhancement for foundation design, please refer to Suen et al. (2025).

3 LOCAL EXPERIENCE OF TEST PILES IN META-SEDIMENTARY ROCKS

3.1 Kowloon-Canton Railway Corporation (KCRC) West Rail Project Phase 1

One of the most extensive test pile program undertaken in Hong Kong could be traced back to 1998 for the Kowloon-Canton Railway Corporation (KCRC) West Rail Project Phase 1, during which a total of 14 numbers of full-scale pile tests were carried out in igneous and MS rocks with various degree of weathering according to Littlechild et al (2000) and Hill et al (2000). The aim of the test piles was to optimise the foundation design so as to save time and cost for the fast-track West Rail project. A total of 2 out of 14 numbers of test piles were tested in MS rocks at Tin Shui Wai. These test piles, namely TSW1 and TSW2, were designed to verify the end-bearing capacity with an effective diameter of 1.2 m and rock socket lengths of 1.6 m and 0.7 m respectively. The test load was applied through a single 850 mm diameter Osterberg cell (O-cell) installed at pile toe combined with the loading kentledge. Similar to the pile construction method at present, the excavation in rock was carried out by the Reverse Circulation Drilling (RCD) apparatus to form the rock socket (see **Plate 1**).



Plate 1: RCD for Construction of Rock Socket for the Test Piles

For the O-cell, a 65 mm thick top and base steel plates were welded to cell prior to welding onto the base section of the reinforcement cage (see **Plate 2**). Grouting beneath and around the O-cell was carried out through 3 sacrificial grout pipes immediately prior to concreting of the pile. The O-cell was instrumented with 3 nos. of displacement transducers to measure the opening of the cell and the hydraulic pressure to operate the cell was monitored through the high-pressure vibrating wire piezometer. Rod extensometers at the top of O-cell (2 nos. per level) and retrievable multi-point borehole extensometer along the pile were installed to monitor the pile movement while vibrating wire strain gauges were installed to monitor the strain at different levels (4 nos. per level). At the pile head, vibrating wire load cells were installed to monitor the applied load through the kentledge while dial gauges were installed to monitor the pile head movement relative to the reference beam (see **Plate 3**). Movement check points were also set at the reference beam to monitor any undue movement of the reference beam during the loading test.



Plate 2: Osterberg Cell at Pile Base



Plate 3: Hydraulic Jacks with Load Cells at Pile Head

3.2 Recent Projects

For the residential projects at Sai Sha, it was proposed to use 813 mm diameter reinforced concrete test bored piles to verify the end-bearing capacity of the founding MS rocks with Rock Mass Rating not less than 45 by a kentledge (SEC Cases 29/2021 and 44/2021). The applied load at the pile base would be monitored by a set of strain gauges near the pile base. When the pile is loaded at the top, the relationship between the applied load and the average strain value can be established. When the same average strain value is measured by the strain gauges at the pile base, it is deemed that the corresponding applied load at the pile base can be determined. The loading kentledge is indeed needed to allow for frictional loss along the pile shaft during the loading test. However, due to the limit of the structural capacity of the pile, the maximum applied load would be limited to about 16,000 kN. The pile details are shown in **Figure 1**. Unfortunately, the test pile has not been proceeded due to tight programme constraint.

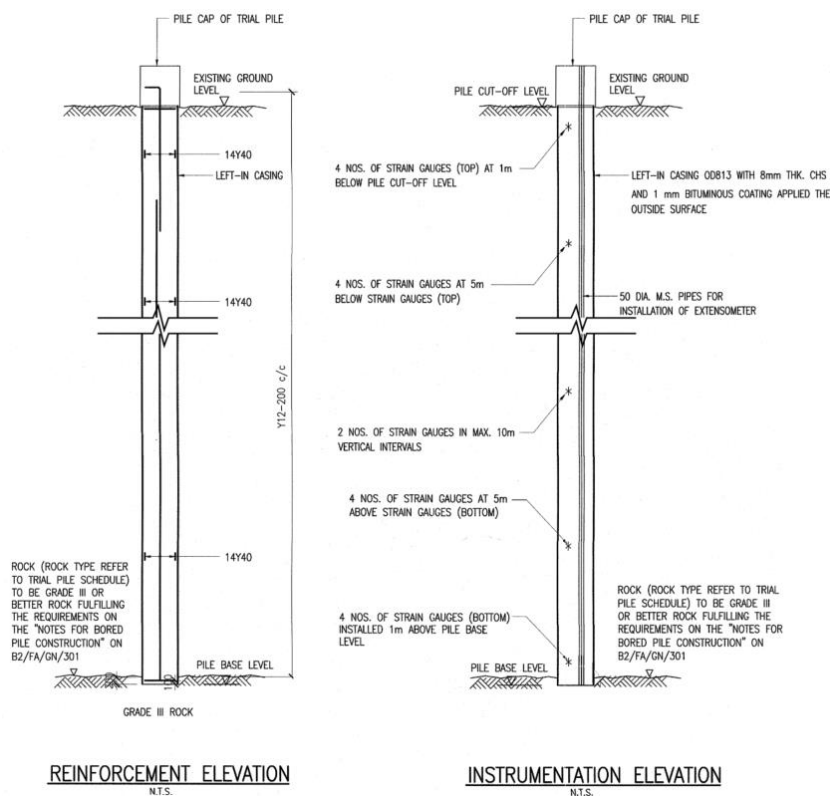


Figure 1: Typical Detail of 813 mm Diameter Test Pile at Sai Sha

Yau et al (2024) reported that full scale load tests on 2 trial piles (with similar set up as the test pile at Sai Sha) with full instrumentations resting on MS rocks with an RMR value above 50 were conducted in Tin Shui Wai. The ultimate bearing pressure of both piles was well in excess of 15,000 kPa. Taking into account of the required factor of safety of 3, the allowable bearing pressure of the site was set at 5000 kPa for rock mass with an RMR value greater than 50.

4 LAUNCHING OF PILE TESTING PROGRAMME IN NORTHERN METROPOLIS

The conservative design parameters for MS rocks can lead to a larger scale and more costly foundation solution, undermining the efficient development of the Northern Metropolis. Because of this, there is a pressing need to improve the current design guidelines with a view to facilitating a more economical yet safe foundation design. In this connection, GEO has initiated a series of full-scale bi-directional pile load tests utilising O-cells in the Northern New Territories (Chik et al. 2025). The first batch of test piles were carried out in trial sites in Yuen Long South (YLS) and Long Bin (LB), with two test piles carried out in each site. Along the pipeline, there

would be more test piles to be carried out in other parts of the Northern New Territories (e.g., Lok Ma Chau, Wang Chau, Sandy Ridge, etc.).

In the following sections, one of the test piles in each site will be presented, including the details of the test setup, loading sequences, and load-displacement behavior. The application of the RMR system for geological characterisation will also be briefly discussed. In addition, the implementation of fibre optic technology for real-time strain monitoring during testing will be evaluated.

5 TEST PILE CONSTRUCTION AND DETAILS

5.1 Use of Osterberg Cells

Full-scale bi-directional pile load tests using O-cells were conducted at trial sites in YLS and LB to investigate the performance of bored piles socketed into MS rocks. The O-cell is a hydraulically driven, sacrificial jack embedded within the pile, which applies force simultaneously in upward and downward directions. This enables separate measurement of shaft resistance and end-bearing resistance when the O-cell is placed at the bottom of the pile, offering direct load transfer mechanisms within the test pile.

Compared with the conventional top-down pile load tests, the bi-directional method offers practical advantages, especially for deep pile with substantial shaft friction contribution. It provides direct load transfer among the end-bearing resistance and the rock socket friction. Importantly, the internal loading arrangement allows the mobilisation of maximum available resistance at both the shaft and base within a single test setup.

5.2 Geological Condition at Test Pile Location

The geological conditions at the location of the two test piles were thoroughly investigated through predrilling before the founding levels of the pile were determined.

At the YLS site, predrill borehole YLS-PD07 encountered a thin fill layer at the ground surface, underlain by the alluvial deposit comprising light grey to brown silty clayey sand and sandy silty clay, with Standard Penetration Test (SPT-N) values ranging from 4 to 16. Completely decomposed metasiltstone and metasandstone (Grade V) were encountered starting from approximately 16.5 m below ground level. The founding stratum for the test pile YLS-P2 was located within the bedrock zone classified as Grade II/III, comprising moderately strong to strong, moderately to slightly decomposed meta-siltstone and meta-sandstone, encountered at an elevation of -36.71 mPD. More than three times the pile base diameter below the pile base, slightly decomposed impure marble (Grade II) without evidence of dissolution features was also observed.

At the LB site, predrill borehole PB01 revealed a stratigraphic sequence beginning with a fill layer of greyish brown to dark brown sandy clayey silt, underlain by a layer of light grey, slightly sandy silty clay Alluvium. Below this, the profile consisted of interbedded layers of meta-siltstone and meta-sandstone spanning weathering Grades II to V. The target founding stratum was identified as Grade II/III metasiltstone, characterised as moderately strong to strong and moderately to slightly decomposed at a depth of more than 85 m below ground level. The test pile LB-P1 was socketed into this stratum, with its base located at -87.01 mPD.

In addition to borehole logging and material classification, the geological conditions at each test pile location were further evaluated using the RMR method. For both test piles, individual ratings for each parameter were determined using a length-weighted average method across the depth of influence. The derived RMR values for YLS-P2 and LB-P1 are summarised in **Table 1**. The derived RMR values provide a quantitative assessment of rock mass quality at different depths, which could be used to establish the correlation between pile capacity and rock mass characteristics.

Table 1: Rock Mass Rating Values for YLS-P2 and LB-P1

Test Pile No.	Strength (≤ 15)	RQD (%) (≤ 20)	Joint Spacing (≤ 20)	Conditions of Joints					Ground-water (7)	Total (≤ 88)
				Discontinuity Length (2)	Separation (≤ 6)	Roughness (≤ 6)	Infilling (≤ 6)	Weathering (≤ 6)		
In rock socket										
YLS-P2	15	14	9	2	1	1	6	5	7	60
LB-P1	12	8	6	2	4	5	6	5	7	55
Within 1 time the pile base diameter below founding level										
YLS-P2	15	20	10	2	1	1	6	5	7	67
LB-P1	9	3	6	2	4	5	6	5	7	47

5.3 Construction Details of Test Piles

At the YLS site, the diameters of the test pile (YLS-P2) were 813 mm diameter in soil and 750 mm in rock socket. Installation involved advancing a steel casing to rockhead using a MAXA STABOTEC Enviro Flush Casing System, followed by rock socket formation with a down-the-hole hammer. YLS-P2 was constructed with a total length of about 47 m and a rock socket length of 0.91 m. In contrast, the test pile in LB site (LB-P1) adopted a larger diameter of 1,500 mm in soil and 1,350 mm in rock socket. It was formed by soil grab excavation inside temporary steel casing down to rockhead followed by socket drilling using the RCD method. LB-P1 has a total length of about 90 m and a rock socket length of 1.5 m. A relatively short rock socket length was deliberately adopted for both test piles to reduce the available socket bond resistance. This design approach aimed to bring the rock/pile interface closer to ultimate conditions, enabling an assessment of the socket's ultimate bond resistance. To minimise the friction along the pile shaft in soil, permanent steel casing was installed from the ground level down to the top of rock socket. This approach helped reduce the load transfer between the pile and the overlying soil during testing, thus allowing a more accurate assessment of the response of the rock socket.

Instrumentation was installed to monitor strain, displacement, and pile behavior throughout the test. Continuous monitoring was carried out to capture the pile response under each load increment. Measurements from multiple instrumentation sources were recorded and managed via a central data logger. Expansion across the O-cell was recorded by four Geokon Model 4450 linear vibrating wire displacement transducers (LVWDTs). Rod extensometer pipes of 13 mm diameter were fixed onto the reinforcement cage to measure displacements at various locations; above the O-cell, below the base plate, and at the top of the rock socket. The head of the rod extensometers were extended to approximately 1 m above pile cap surface, and additional LVWDTs were installed at the top of the pile cap to monitor the extrusion of the rod extensometers' head throughout the load test. Rebar strainmeters Geokon Model 4911, commonly known as the "Sister Bars" (see **Plate 4**) were positioned in multiple levels along the pile shaft to capture strain profiles. The rebar strainmeter was designed to integrate into the pile by tying it alongside the rebar cage. As the strain behavior near the pile base and within the rock socket was of particular interest, denser instrumentation was employed in that region. The rebar strainmeters were arranged in four-gauge arrays from 1 m above the rock socket down to the pile base with nominal 500 mm interval, and in two-gauge arrays from the pile head to just above the rock socket at nominal 8 m interval. Apart from conventional strain gauges, a fibre optic distributed sensing system was employed to capture real-time strain and temperature data along the pile, providing an extra layer of spatially distributed sensing for verifying strain gauge trends or detecting unexpected responses. In addition, pile head movements were measured by a pair of Leica NA3000 digital levels to a precision of 0.01 mm, with observations taken at fixed backsights and foresights throughout the test. The instrumentation elevation plans for YLS-P2 and LB-P1 are shown in **Figures 2 and 3**, respectively.



Plate 4: Rebar Strainmeter

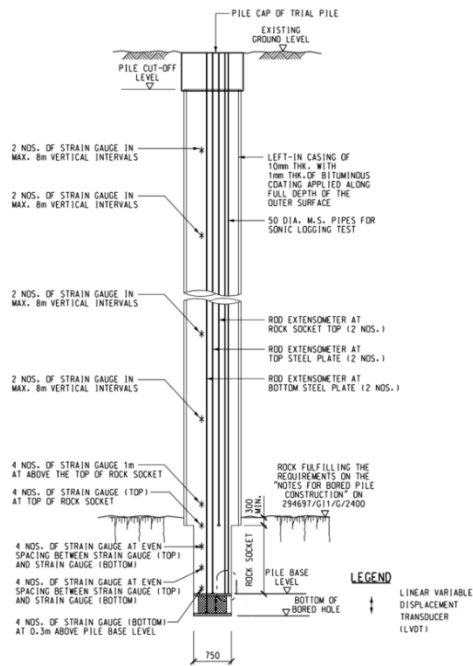


Figure 2: Instrumentation Elevation for YLS-P2

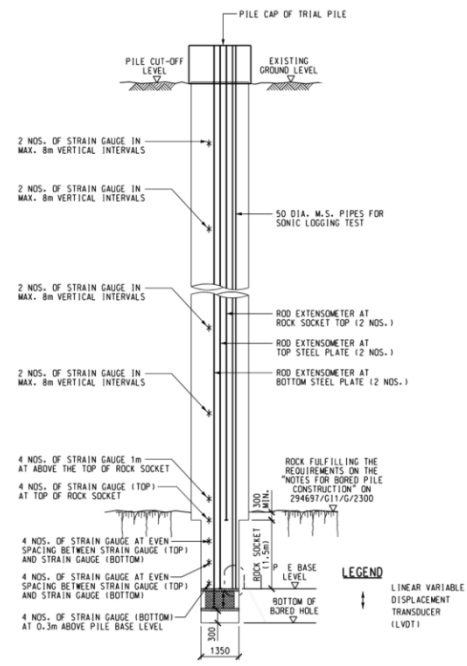


Figure 3: Instrumentation Elevation for LB-P1

The O-cell assemblies were embedded into the reinforcement cages with 50 mm steel bearing plates welded above and below the O-cell to transmit load in opposing directions – upwards to mobilise shaft friction and downwards to mobilise end-bearing resistance. At YLS, a single O-cell with a diameter of 530 mm and a maximum jacking capacity of 10 MN was installed at the pile base. This was paired with 560 mm diameter bearing plates designed to ensure uniform load transfer, with the bottom plate placed in direct contact with the founding rock mass. On the other hand, a higher-capacity setup was adopted in LB, utilising five horizontally arranged O-cells, each 430 mm in diameter and rated to 6.4 MN, yielding a combined jacking capacity of approximately 32 MN. These were installed near the pile base and coupled with steel bearing plates of 1,235 mm in diameter to match the wider pile geometry. Given that such pile was constructed with RCD which typically resulted in a non-uniform rock socket base, a nominal 300 mm thick concrete bedding layer was placed beneath the bottom bearing plate to ensure full and uniform engagement between the pile base and the founding rock mass. To facilitate the placement of this bedding layer, a 300 mm diameter hole was reserved at the centre of the steel bearing plates, allowing insertion of a tremie pipe down to the base of the rock socket. **Plates 5 and 6** demonstrate the O-cell assembled with steel bearing plates and reinforcement cages for YLS-P2 and LB-P1, respectively. **Plate 7** presents the underside of the bottom steel bearing plate installed for LB-P1.



Plate 5: O-cell Assembly for YLS-P2



Plates 6: O-cell Assembly for LB-P1



Plate 7: Underside of Bottom Steel Plate for LB-P1

Both configurations incorporated O-cells with a stroke of 225 mm, allowing sufficient displacement to fully mobilise end-bearing resistance and shaft friction. The hydraulic pressure required to operate the O-cells was delivered via air-driven pumps, using water as the hydraulic medium. This substitution of oil with water not only aligned with environmental protection standards but also mitigated the risk of contamination in the event of leakage during testing. The typical set up for the hydraulic pumps for the O-cell is shown in **Plate 8**.



Plate 8: Set Up of the Hydraulic Pumps for O-cell

5.4 Procedures of Load Testing

The test piles were loaded in a series of cycles with progressively increasing applied load at the O-cell, as shown in **Table 2**.

Table 2: Test Cycles and Maximum Applied Loads

Cycles	Max. Test Load (% of a reference pressure of 7,500 kPa)	Max. Test Load at Pile Base (kN)	
		YLS-P2	LB-P1
1	100%	3,317	10,737
2	200%	6,633	21,473
3	300%	9,950	32,210
4	Up to the practical limit of the O-cell		

The target maximum test load was set to achieve an equivalent pressure of 22,500 kPa at the pile base, corresponding to three times the reference pressure of 7,500 kPa. The loading sequence comprised three primary cycles: Cycle 1 reached 100% of the reference pressure (7,500 kPa), Cycle 2 reached 200% (15,000 kPa), and Cycle 3 reached 300% (22,500 kPa). For each 50% load increment, the holding period continued until the rate of displacement fell below 0.05 mm over a 10-minute interval, sustained for at least 30 minutes. At the maximum test load of 22,500 kPa, a prolonged hold period of 72 hours was adopted to capture time-dependent movements and assess long-term pile behavior under high stress.

At the end of each unloading cycle, residual settlement was recorded to capture the extent of unrecoverable displacement. Following the completion of Cycle 3, an additional Cycle 4 was introduced to further increase the applied load beyond the initial target, with the aim of examining the pile response under extreme loading conditions. For YLS-P2, the maximum test load achieved during Cycle 4 was 390% of the reference pressure, while for LB-P1, the peak load reached was approximately 340%. As Cycle 4 was not part of the original testing objective, only the results from Cycles 1 to 3 are presented and discussed in this paper.

At the start of the test, loading commenced without restraining the pile head – meaning that the pile head was not engaged to any loading kentledge to allow free upward movement when the O-cell was expanded. Under such unrestrained condition, the applied load in the O-cell was resisted by a combination of base resistance and shaft friction along the entire pile, including both the soil shaft and rock socket. This unrestrained phase was designed to assess the mobilised shaft friction, particularly within the rock socket. To ensure that the rock socket resistance could be largely mobilised before the end-bearing resistance became dominant, the test piles were deliberately constructed with relatively short rock socket lengths. Once the available shaft friction was insufficient to counteract the applied load, the expansion of the O-cell could rapidly become excessive. To preserve sufficient O-cell stroke for full load application to the pile base in subsequent loading cycles, two predefined trigger conditions were established to safeguard the test setup: (i) if the O-cell stroke exceeded 80 mm, or (ii) if the upward displacement measured at the top of the rock socket exceeded 4% of the socket diameter. If either condition was met during loading, the test would be paused immediately to turn into restrained phase. The O-cell would be unloaded to zero, and the loading kentledge would be engaged before reloading of the O-cell. These criteria were carefully defined to allow the rock socket friction to be fully mobilised during the unrestrained phase (usually ~ 1 to 2% of the socket diameter), while still preserving adequate O-cell stroke for mobilising the end-bearing resistance in the restrained phase. Given that the maximum allowable stroke of the O-cell was 225 mm, the 80 mm threshold was considered adequate.

The purpose of the loading kentledge system is to restrain the upward movement of the pile head, thereby enabling the full development of the end-bearing resistance. At the pile head, hydraulic jacks were installed to apply a seating load, ensuring full engagement between the pile and the kentledge system at the beginning of the restrained phase. Load cells were used to monitor the load transferred onto the kentledge. When 90% of the kentledge load was mobilised, the test would be ceased for safety concern. **Plate 9** presents the hydraulic jacks with load cells installed at the pile head at LB-P1.



Plate 9: Hydraulic Jacks with Load Cells at Pile Head at LB-P1

The minimum kentledge weights adopted were 10 MN for YLS and 30 MN for LB, in line with the anticipated maximum test loads and overall safety requirements for restrained testing. Conversely, if neither trigger condition was reached throughout all planned load cycles, it would indicate that the shaft friction was sufficient to balance the applied load at the O-cell, and the engagement of the kentledge system would not be required. This was the case for YLS-P1, where the test completed without the need to activate the kentledge system. In contrast, LB-P1 had experienced failure in the shaft friction. During Cycle 3 of the unrestrained phase, the loading was halted at an applied load of approximately 30 MN ($\sim 280\%$ load) when the pressure started to drop and failed to be maintained. Although the top plate movement at that moment was just around 10 mm which had not reached any trigger conditions, it was considered that the shaft friction had been fully mobilised. The pressure continued to drop until an approximate 35 mm upward movement was recorded. The behavior indicated that the available shaft friction was insufficient to counteract the applied load at the O-cell. The unrestrained phase was then suspended with the O-cell unloaded, and the kentledge system was engaged to allow further loading under restrained conditions.

6 DISCUSSION OF PRELIMINARY LOAD TEST RESULTS

6.1 Load & Movement Behavior

For YLS-P2, the pile base was loaded up to 10,030 kN, which corresponded to slightly above 300% of the reference end-bearing pressure (three times of 7,500 kPa). As illustrated in **Figure 4**, the load-settlement behavior for YLS-P2 demonstrated that at this load level, the corresponding settlement recorded at the bottom plate was 3.91 mm. Notably, during the initial stage of loading, a disproportionately large settlement of 2.03 mm occurred during the first 50% load increment. This behavior deviated from the more gradual settlement trend typically expected in early loading stages and was likely attributed to initial seating effects at the pile base. As discussed in Section 5.3, YLS-P2 was constructed with the bottom steel plate placed directly on the founding rock. The observed seating effects may have resulted from local compression of the slightly uneven rock surface beneath the base plate. Subsequent load increments exhibited smaller and more consistent trend of displacements, indicating that the initial seating had stabilised in the loading process.

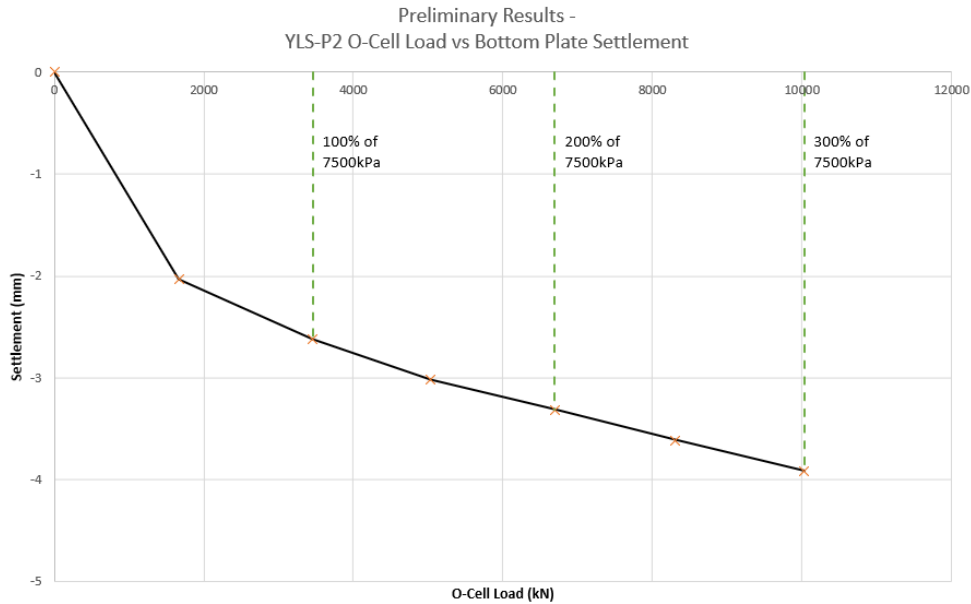


Figure 4: O-cell Load against Bottom Plate Settlement of YLS-P2

For LB-P1, the pile was loaded up to 32,260 kN under the restrained phase, which corresponded to 300% of the reference end-bearing pressure (three times of 7,500 kPa). The load-settlement behavior for YLS-P2 is illustrated in **Figure 5**. The settlement recorded at the bottom plate was 11.53 mm at this load. Unlike YLS-P2, this pile did not exhibit an abnormally large settlement during the initial loading stage. Instead, the overall trend of base settlement remained steady, with the rate of settlement gradually increasing as the applied load intensified. This behavior may be attributed to the presence of a concrete bedding layer beneath the bottom bearing plate, which provided a more uniform interface between the bottom plate and the founding rock. The bedding layer likely helped distribute stress more evenly, reducing localised deformation and minimising seating effects typically associated with direct contact on uneven rock surfaces.

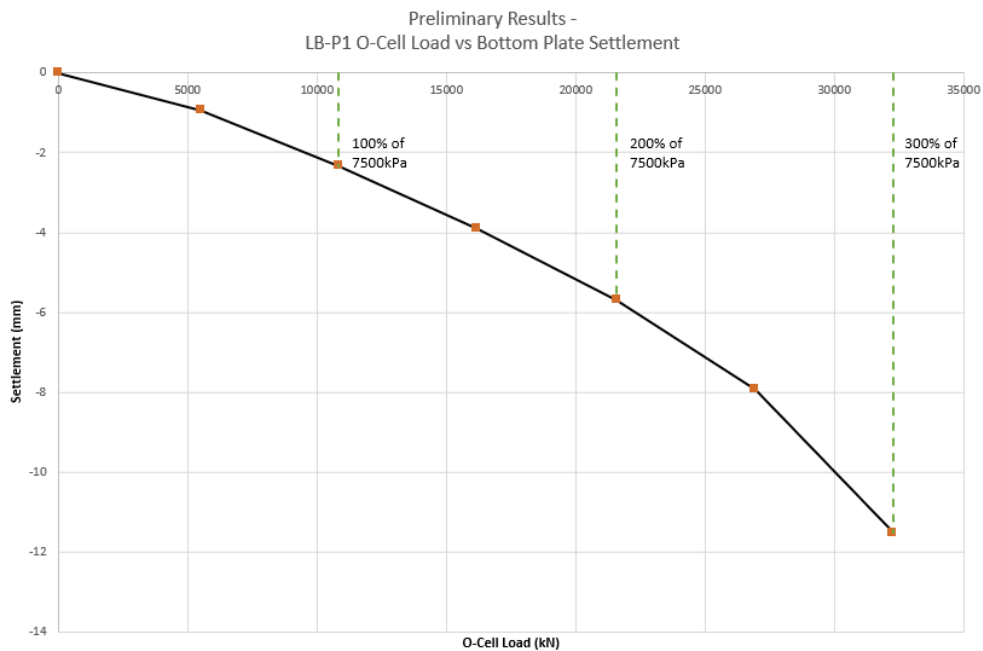


Figure 5: O-cell Load against Bottom Plate Settlement of LB-P1

The mobilised end-bearing resistance derived from the O-cell load and the corresponding settlement of the bottom plate are summarised in **Table 3**. The settlement values were normalised with respect to the pile base diameter to facilitate comparison across different pile sizes. For instance, at 300% load, YLS-P2 achieved an end-bearing pressure of 22,703 kPa with a bottom plate settlement of 3.91 mm (0.52% of rock socket diameter). In contrast, LB-P1 resulted in larger settlements under similar pressure level. The bottom plate settlement at LB-P1 reached 11.53 mm (0.85% of pile socket diameter) under an end-bearing pressure of 22,538 kPa. The larger movements in LB-P1 suggest a more compressible rock stratum beneath the pile base as compared to YLS-P2. Overall speaking, the settlement at one time the reference pressure (7,500 kPa) was found to be less than 1% of the pile base diameter, while the settlement at three times the reference pressure remained below 3% of the pile base diameter.

Table 3: Summary of Mobilised End-Bearing Resistance up to 300% Reference Pressure

Pile No.	Pile Diameter (mm) pile shaft / rock socket	Mobilised End-Bearing Resistance (kPa)	Bottom Plate Settlement (mm) / % of Rock Socket Diameter
YLS-P2	813 / 750	7,832	2.62 / 0.35%
		22,703	3.91 / 0.52%
LB-P1	1500 / 1350	7,524	2.33 / 0.17%
		22,538	11.53 / 0.85%

The test was carried out beyond 300% of the reference pressure, reaching the practical loading limit of the O-cell. During the test, a maximum mobilised end-bearing resistance of approximately 29,000 kPa and 25,000 kPa for YLS-P2 and LB-P1 has been reached respectively, without significant further bottom plate settlement.

These findings indicated that both test piles exhibited relatively stiff end-bearing responses, with limited deformations even under high load levels. The normalised settlement values fell within acceptable performance ranges commonly referenced in local and international design practices, suggesting that the founding MS rocks possessed favorable bearing characteristics. This supports the potential for adopting higher end-bearing design values.

6.2 Young's Modulus of Rock Mass

The Young's modulus of the rock mass (E_m) is a critical parameter for estimating settlement of piles founded on rock. For piles founded on rock, the settlement at the surface of the rock mass can be calculated by the following formula assuming a homogeneous elastic half space below the pile tip:

$$\delta_b = \frac{q(1 - \nu_r^2)D_b}{E_m} C_d C_s$$

where δ_b = settlement at the surface of the rock mass; q = bearing pressure on the rock mass; C_d = depth correction factor; C_s = shape and rigidity correction factor; ν_r = Poisson's ratio of rock mass; D_b = pile base diameter and E_m = Young's modulus of rock mass.

Focusing on the working load range and to mitigate the effects of seating load settlement, the Young's modulus was calculated using the bottom plate settlements between 100% and 200% of the reference pressure. For YLS-P2, with a settlement of 2.62 mm at 100% and 3.31 mm at 200%, the back-calculated E_m value is 10.49 GPa. For LB-P1, with a settlement of 2.33 mm at 100% and 5.70 mm at 200%, the E_m value is 3.85 GPa. These calculated Young's modulus values have been compared and found roughly consistent with the previous test pile results from Figure 6.7 of GEO (2006).

7 DISCUSSION OF FIBRE OPTIC TECHNOLOGY FOR STRAIN MEASUREMENTS

7.1 Use of fibre optic technology for real-time strain measurements

This project adopts distributed fibre optic sensing technology for strain measurements during the load tests. Recent years have seen advances and applications of various types of fibre optic technology in civil engineering instrumentation, including the use of fibre Bragg grating (FBG) sensors or Brillouin optical time domain reflectometry (BOTDR) technology. This study adopts the optical frequency domain reflectometry (OFDR) technology. Compared with FBG and BOTDR, OFDR sensing system can achieve a higher spatial resolution of strain measurements with high sensing frequency for dynamic or real-time strain measurements.

The OFDR sensing technology is based on Rayleigh scattering (Lin et al. 2023). Light output from a tunable laser source in the OFDR equipment is divided into two parts by an optical coupler, with one part used as the reference light and the other used as the measurement light. When the measurement light propagates in the fibre optic cable, backscattered light is generated due to inhomogeneity in the refractive index of the optical fibre. This backscattered light is transmitted back to the equipment and then mixed with the reference light by the optical coupler. The resulting coherent interference is received and demodulated by the photoelectric detector to obtain the strain and/or temperature change along the sensing cable, which is related to the Rayleigh spectral shift by:

$$\Delta\nu_R = c_\epsilon\Delta\epsilon + c_T\Delta T$$

where $\Delta\nu_R$ = Rayleigh spectral shift; $\Delta\epsilon$ = mechanical strain change of the fibre optic cable; ΔT = temperature change; c_ϵ = coefficient of Rayleigh frequency shift induced by mechanical strain change (= $-0.15 \text{ GHz}/\mu\epsilon$; and c_T = coefficient of Rayleigh frequency shift induced by temperature change (= -1.25 GHz/K).

Since $\Delta\nu_R$ is influenced by changes in both strain and temperature, it is necessary to single out the temperature effects by another loose tube fibre optic cable, where the outer sheath is not mechanically bonded to be fibre optic core. For these cables, the measured $\Delta\nu_R$ only arises from ΔT . Therefore, two types of fibre optic cables were utilised and they were both manufactured by NanZee Sensing Technology in Suzhou, China. The strain and temperature sensing cables are referred to as NZS-DSS-C02 and NZS-DTS-C05 cables, respectively. **Figure 6** (Lin et al. 2023) shows the schematic diagrams of the cross sections of these cable types. NZS-DSS-C02 is a type of metal-based funicular strain sensing cable, which is single mode and uses multi-strand metal reinforcement to improve the surface strength of the sensing fibre. The metal reinforcement enhanced its robustness, making it more versatile in construction site environments. The diameter (D) of the cable adopted in this project is 5.0 mm and its weight is 38 kg/km. NZS-DTS-C05 is a type of plastic package armoured cable for temperature measurement, where strain transfer is prevented by a void between the sleeve and the fibre core. Its diameter is about 5.0 mm with an operational range of is from $-20 \text{ }^\circ\text{C}$ to $85 \text{ }^\circ\text{C}$.

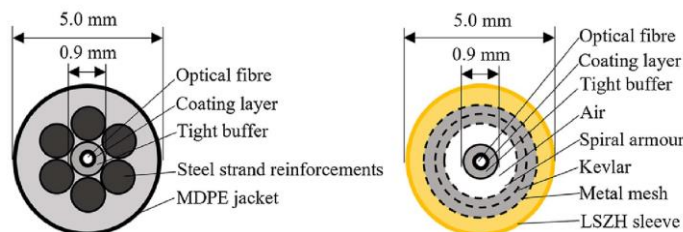


Figure 6: Fibre optic cables for strain and temperature measurements: (left) NZSDSS-02 cable; (right) NZSDSS-05 cable (adapted from Lin et al 2023)

The equipment used in the load tests was LUNA ODiSI 6102 fibre optic sensing interrogator. It has a maximum spatial resolution of 0.65 mm for strain and temperature measurements. The spatial resolution is adjustable, and for applications in field pile load tests it is typical to adopt the resolution of 1 to 2 cm. During field deployment, the fibre optic cables were mounted onto the longitudinal reinforcement bars along the

reinforcement cage, and fixed by plastic cable ties. No pre-straining operation was conducted for the fibre optic cables, as they were expected to be fully embedded in reinforced concrete and hence experience the same strains as the pile material.

7.2 Comparison between fibre optic technology and vibrating wire strain gauges

Figure 7 shows the strain measurements at YLS-P2, obtained by optical fibre sensors after compensating for temperature effects. The data from two cables are plotted together with the average value, at different load stages up to around 9,950 kN. As the Osterberg cell applies an upward load from near the pile tip, compressive strains are induced with maximum values close to the bottom and reduce with elevation. The corresponding data obtained by vibrating wire strain gauges are also plotted for comparison. In general, the strain gauge and fibre optic data match with each other. Such variations of strains at the same elevation might be due to eccentricity of the applied load.

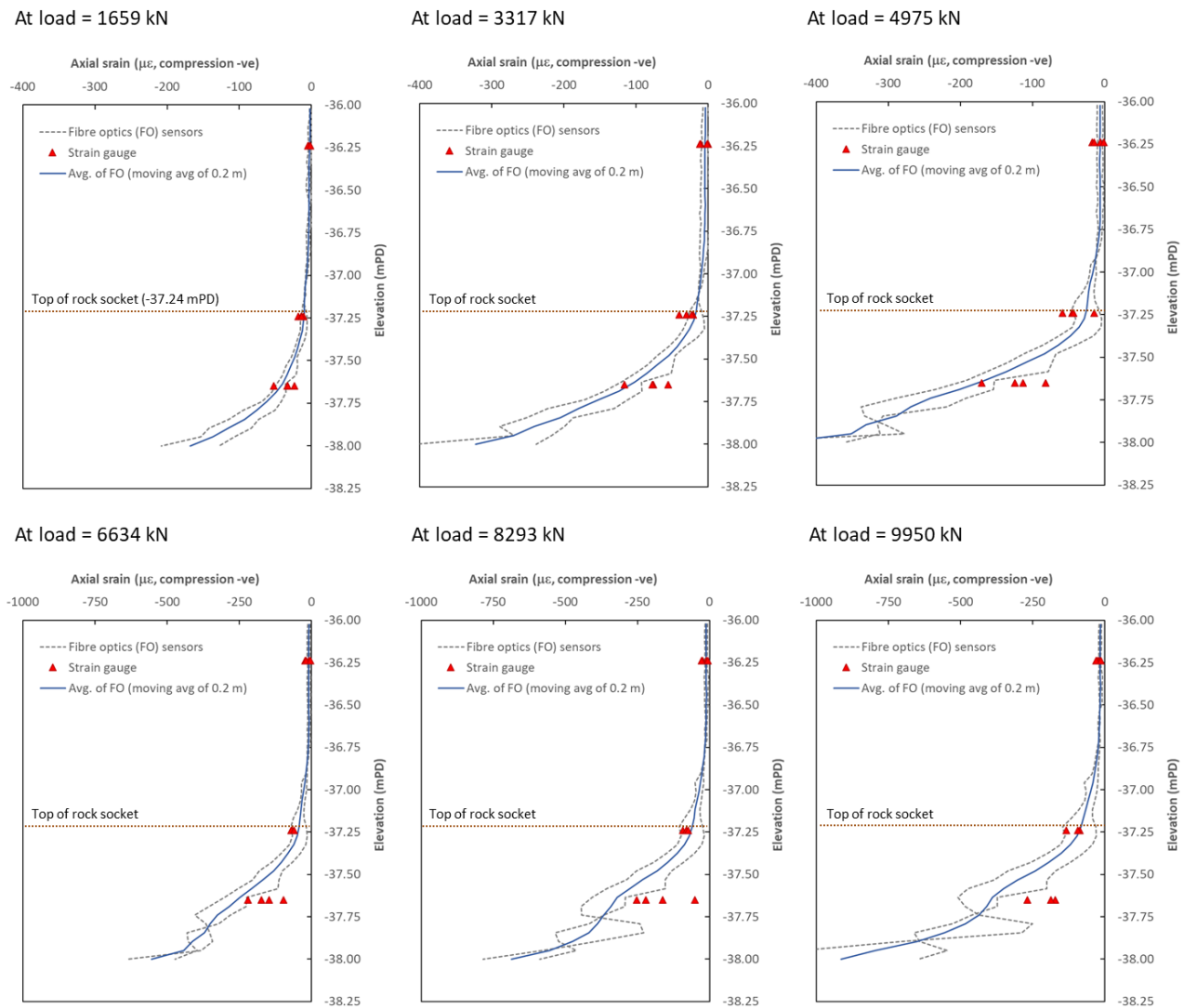


Figure 7: Fibre Optic Strain Measurements Compared with Strain Gauge Data for YLS-P2

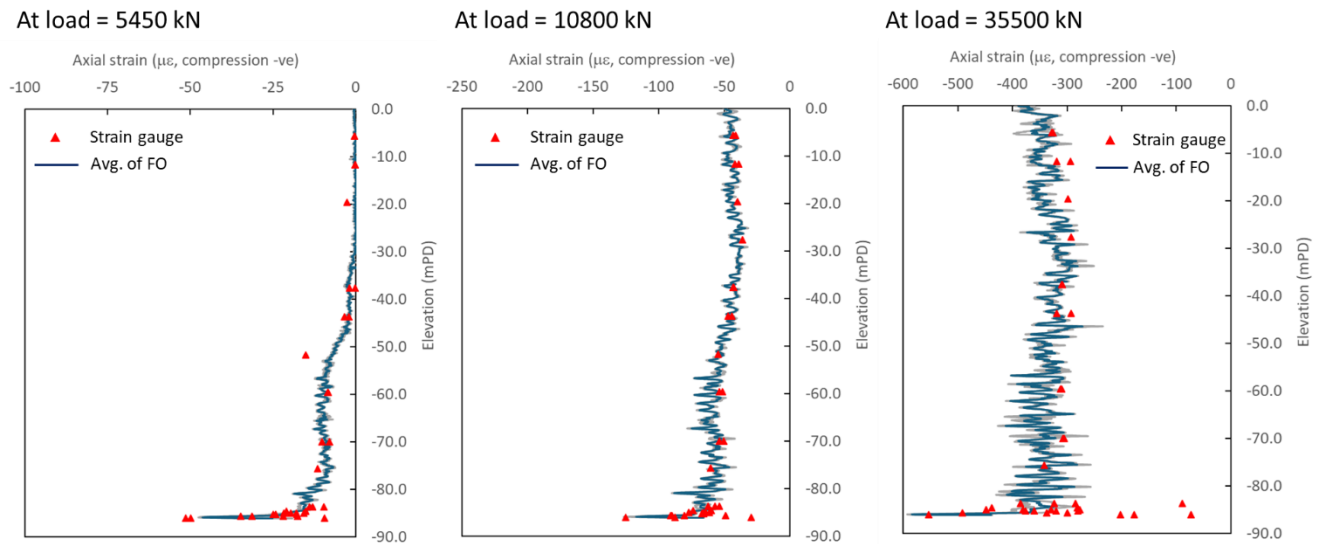


Figure 8: Fibre optic strain measurements compared with strain gauge data for LB-P1

8 CONCLUSIONS

The full-scale bi-directional pile load tests conducted at Yuen Long South and Long Bin have provided valuable, high-quality data on the performance of bored piles socketed into MS rocks in the northern New Territories. Through the use of Osterberg Cells and comprehensive instrumentation including both vibrating wire strain gauges and fibre optic sensors, this study has enabled direct measurement of shaft friction and end-bearing resistance, as well as detailed assessment of load transfer mechanisms and settlement behavior.

Importantly, the mobilised end-bearing capacities and observed settlements from these tests are consistent with, and in some cases exceed, the recommended allowable bearing pressures for jointed rock masses as set out in the Figure 6.8 of GEO (2006). The test results may substantiate the use of higher bearing pressures than those typically adopted in conservative design, subject to further upcoming test piles in other parts of the Northern New Territories.

The successful application of fibre optic technology for real-time strain monitoring, alongside traditional instrumentation, has also been demonstrated, offering enhanced spatial resolution and operational efficiency for future testing programs.

In summary, this study provides strong evidence that pile design in MS rocks can be optimised by integrating detailed geological assessment and full-scale pile load testing. The findings support a leap towards more economical and reliable foundation solutions for major infrastructure and urban development projects in Hong Kong, particularly within the context of the Northern Metropolis.

ACKNOWLEDGEMENTS

This paper is published with the permission of the Head of the Geotechnical Engineering Office and the Director of Civil Engineering and Development, the Government of the Hong Kong Special Administrative Region of the People's Republic of China.

REFERENCES

- BD (2024). *Code of Practice for Foundations 2017 (2024 Edition)*. Buildings Department, Hong Kong.
- Bieniawski, Z.T. (1974). Geomechanics classification of rock masses and its application in tunnelling. *Proceedings of the Third International Congress of the International Society for Rock Mechanics*, Denver, vol. 2A, pp 27-32.
- Bieniawski, Z.T. (1989). *Engineering Rock Mass Classification*. John Wiley, New York, 251 p.

- Chik, S.S.W., Chiu, K.Y.K., Lau, R.W.Y., Chau, A.Y.L., Sze, E.H.Y., Wong, P.P.C., Hui, T.H.H. (2025). Trial Piles and Foundation Design in Meta-sedimentary Rocks. *Proceedings of the 45th Annual Seminar*. Geotechnical Division, Hong Kong Institution of Engineers.
- GEO (2006). *Pile design and construction GEO Publication No.1/2006*. Civil Engineering Department, Hong Kong.
- GEO (2023). *Supplementary Guidelines for Foundation Design and Construction, GEO Technical Guidance Note No. 53*, Geotechnical Engineering Office, Civil Engineering and Development Department, Hong Kong.
- Hill, S.J., Littlechild, B.D., Plumbridge, G.D. & Lee, S.C. (2000). End bearing and socket design for foundations in Hong Kong. *Proceedings of the 19th Annual Seminar*, Geotechnical Division, Hong Kong Institution of Engineers, pp 167-178.
- Lin, S.Q., Tan, D.Y., Leung, Y.F., Yin, J.H., Li, I., Sze, E.H.Y., Lo, F.L.C., Kan, H.S., Wong, T.C.W. and Chan, E.Y.M. (2023). Fibre optic monitoring of a twin-circular shaft excavation: developments of circumferential forces and bending moments in diaphragm wall. *Journal of Geotechnical and Geoenvironmental Engineering*, Vol. 149 (12), 04023117
- Littlechild, B.D., Hill, S.J., Statham, I. & Plumbridge, G.D. (2000). Stiffness of Hong Kong rocks for foundation design. *Proceedings of the 19th Annual Seminar*. Geotechnical Division, Hong Kong Institution of Engineers, pp 181-190.
- Suen, M.H.Y., Chow, C.C.F., Lau, R.W.Y., Chau, A.Y.L., Wong, P.P.C., Hui, T.H.H. (2025). Evaluation of RMR for Meta-Sedimentary Rocks in Hong Kong: Challenges and Potential Solutions. *Proceedings of the 45th Annual Seminar*. Geotechnical Division, Hong Kong Institution of Engineers.
- Yau, T.L.Y. & Lau, C.K. (2024). Review on the End Bearing Capacity of Large Diameter Bored Piles founded on Meta-sedimentary Rock in Hong Kong. *Proceedings of the Forty-fourth Annual Seminar*. Geotechnical Division, Hong Kong Institution of Engineers, pp 374-385.